Crack Growth Simulation at Welded Part of LNG Tank

Kazuhiro Suga,[a,*] Takafumi Endo,[b] and Masanori Kikuchi[c]

[a)]*Mechanical Engineering, Tokyo University of Science,Suwa, Japan*
[b)]*Mechanical Engineering, Faculty of Science and Technology, Graduate School of Tokyo University of Science, Japan*
[c)]*Mechanical Engineering, Faculty of Science and Technology, Tokyo University of Science, Japan*

*Corresponding author: endo@me.noda.tus.ac.jp

ABSTRACT

The objective of this research is to evaluate crack growth behavior from a surface crack to a through crack in a liquefied natural gas (LNG) tank. Crack growth behavior is analyzed by superposition version FEM (S-FEM). As a crack grows, part of the local mesh crosses over the global mesh. In S-FEM, the local mesh is defined as existing in the global mesh. When a part of the local mesh crosses over the global mesh, the Young's modulus of the part is made small to ignore the influence of the part. In this way, the stress distribution of the local mesh is improved. In this study, crack growth behavior under a tensile cyclic load is analyzed. After crack penetration, the crack shape becomes rectangular. Crack growth behavior under tensile bending loading is also analyzed by simulating the four-point bending test. In this simulation, the crack shape becomes trapezoidal after penetration.

KEY WORDS: *Fatigue Crack; S-version FEM; Surface Crack; Through Crack*.

1.0 INTRODUCTION

A tank storing liquefied natural gas (LNG) has many welded parts. So, in the design phase of the tank, it is necessary to prevent LNG leaking due to fatigue, which can generate a through crack. Crack growth behavior at the welded part under tensile cyclic loading or bending has been researched [1,2,3,4]. However, crack growth behavior at the welded part under tension and bending has not been researched. In this study, the superposition version finite element method (S-FEM) [5,6,7] is used to analyze crack growth behavior under tensile bending loading.

In S-FEM simulation, the global mesh represents the whole structure and the local mesh represents a local part of the structure that has a crack. The displacement function of the local mesh is defined as existing in the global mesh. The case that the local mesh crosses over the global mesh has not been extensively investigated, although one study applied S-version FEM when a local mesh crosses over a global mesh [8].

This research investigates the effects of part of a local mesh crossing over a global mesh on the stress distribution and the stress intensity factor. To show the effects, Young's modulus of the local part is set as E/100. Then, the crack growth process under tensile cyclic loading is simulated. Finally, the crack growth process from a surface crack to a through crack at a welded part under tensile bending loading is simulated.

2.0 NUMERICAL ANALYSIS

To analyze crack growth behavior, S-version FEM is used. The stress intensity factor is calculated by the virtual crack closure-integral method (VCCM) [9].

3.0 PROBLEM OF LOCAL MESH CROSSING OVER GLOBAL MESH

3.1 Conditions of numerical simulation

When a part of the local mesh crosses over the global mesh, the effects on the stress distribution and stress intensity factor are studied. The simulation model is a plate, as shown in Figure 1. The material used in the analysis is aluminum alloy A2017. The thickness of the plate is 2.3 mm. In Figure 1, the left side is the model, and the right side is view from z axial direction. The area enclosed by the green line is the global mesh and that enclosed by the blue line is the local mesh. The red area indicates the initial

crack shape. The plate has a crack of crack depth 2.0 mm and aspect ratio 1.0.

Two cases are simulated by changing Young's modulus in the local mesh that crosses over the global mesh. One case assumes E/100 as the Young's modulus. The other case uses E as the Young's modulus. A cyclic load is applied to the plate, and the stress range is assumed to be 10 MPa.
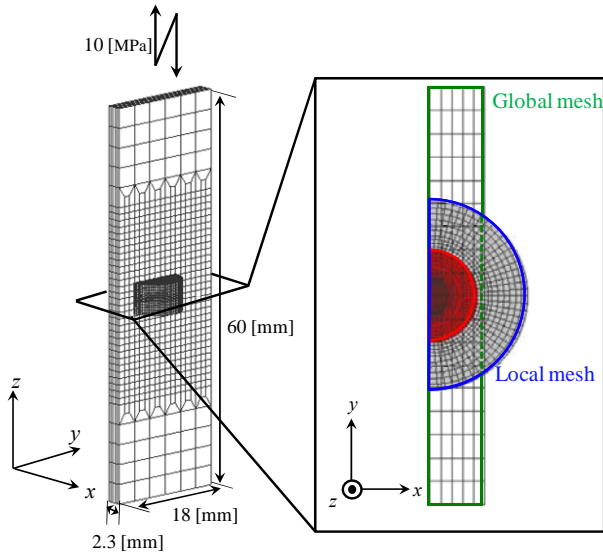
Figure 1: Geometry of plate

3.2 Analysis result
The stress distributions are shown in Figure 2(a) and Figure 2(b). Figure 2(a) is the cross-sectional view of the cracked plane. In Figure 2(b), the x-axis is defined as the direction of the arrows in Figure 2(a). The y-axis is the stress of each direction at the Gauss point of blue area of Figure 2(a). When Young's modulus is E, each stress distribution is negative near the boundary between the global mesh and the local mesh. However, by assuming a Young's modulus of E/100, each stress distribution is approximately 0 MPa.
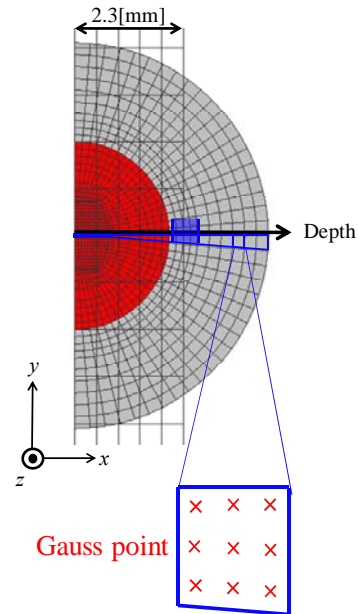
Figure 2: (a) Cross section
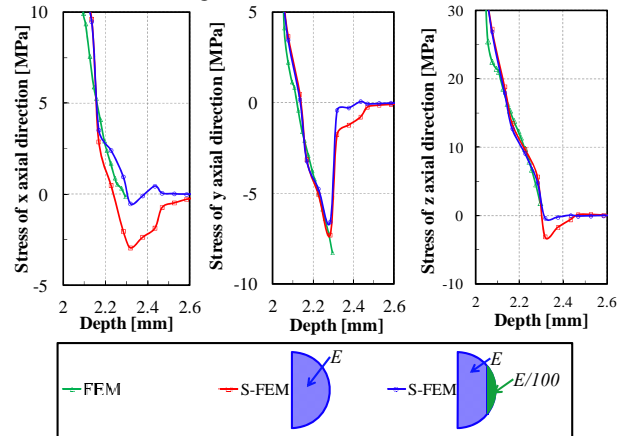
Figure 2: (b) Stress distribution

The stress intensity factors of the two S-FEM cases and the global FEM are shown in Figure 3. The stress intensity factors of the FEM and S-FEM cases are close to each other.
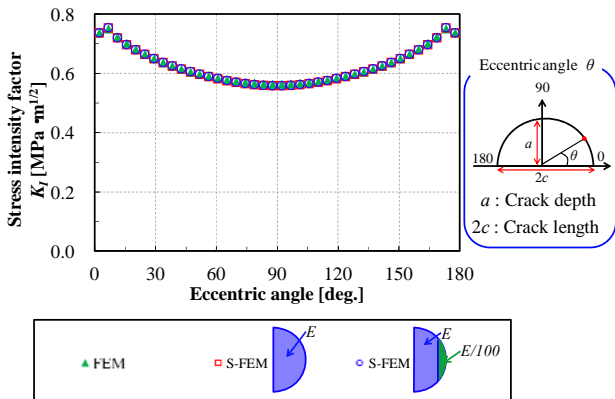
Figure 3: Stress intensity factor
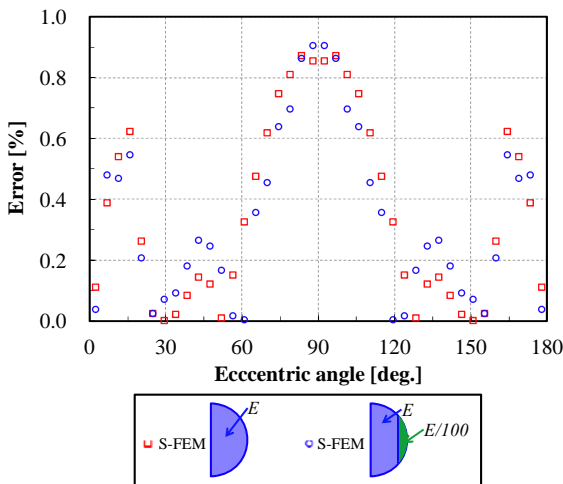
Figure 4: Errors of stress intensity factor between S-FEM and FEM

Assuming that the stress intensity factor of FEM is correct, errors of the stress intensity factors between S-FEM and FEM are shown in Figure 4. The change of Young's modulus does not affect the stress intensity factor, even if the local mesh crosses over the global mesh. So, even if the local mesh crosses over the global mesh, it is clear that the stress intensity factor is calculated accurately. By using this calculation method, crack growth behavior under tensile cyclic loading is analyzed. The crack growth behavior is also analyzed because the stress distribution is improved by assuming that the Young's modulus is E/100.

4.0 CRACK GROWTH BEHAVIOR UNDER TENSILE CYCLIC LOADING

4.1 Numerical model

The crack growth behavior from a surface crack to a through crack under tensile cyclic loading is analyzed. The numerical model is a plate like the one in Figure 5. The right figure is the cross-section view at the crack plane. The red line represents the initial crack. The initial crack shape is semi-elliptical, the crack length is 1.8 mm and the aspect ratio is 0.9. The plate is subjected to a tensile cyclic loading of 80 MPa. The material used in the

analysis is also aluminum alloy A2017.

The crack growth magnitude is calculated by Paris' law (equation (1)) [10]. In eq.(1), C is 1.314×10^{-10} and n is 2.37 (unit: $MPa\sqrt{m}$). In eq.(1), da is crack growth magnitude , dN is Number of cycles and $\triangle K_I$ is Stress intensity factor range.

$$da / dN = C(\triangle K_I)^n \qquad (1)$$
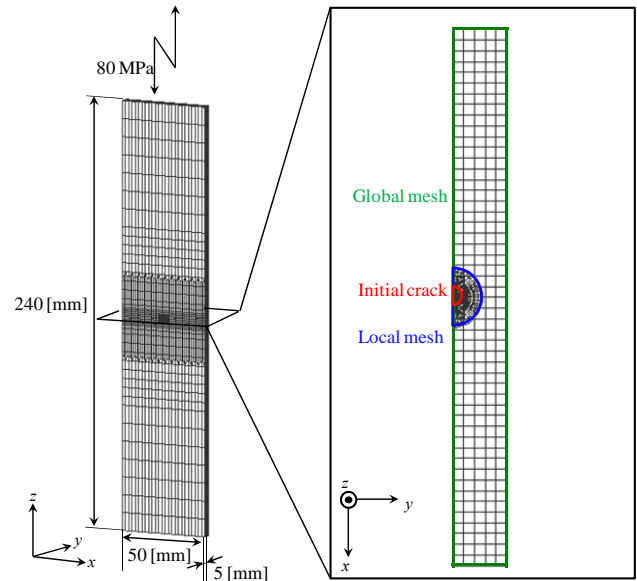
Figure 5: Dimension of plate model

4.2 Result of numerical simulation

Figure 6 shows the changes in crack shapes before penetration. As the crack grows, the crack growth rate increases. Figure 7 represents the changes in the stress intensity factor before penetration. When the number of cycles is 1.01×10^6, the difference of stress intensity factors near the surface becomes large.
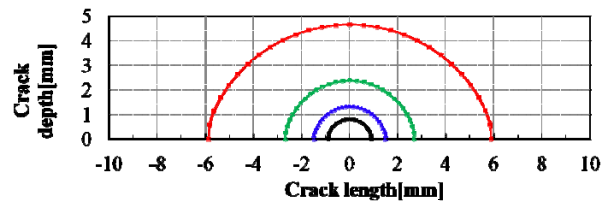
Figure 6: Changes in crack shape before penetration
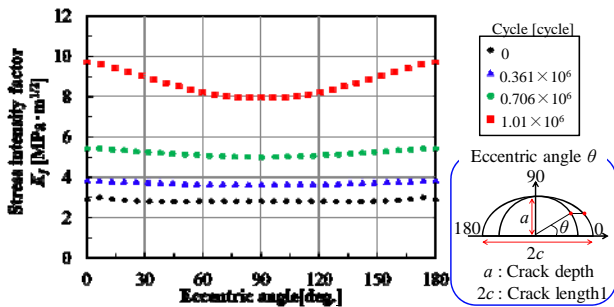
Figure 7: Changes in stress intensity factor before penetration

Figure 8 represents the relation between the aspect ratio and the crack depth. T is the thickness of the plate and a is the crack depth. As the crack grows, the aspect ratio decreases gradually and becomes approximately 0.8. This is the same result found in Lin's [11] and Hosseini's [12] studies.
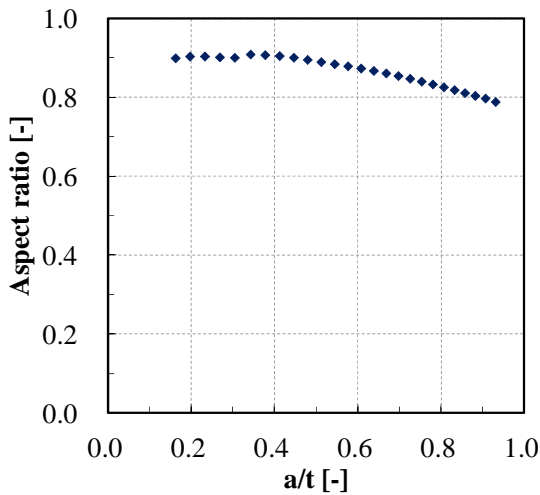
Figure 8: Changes in aspect ratio

Based on the final crack shape before penetration, where the crack depth is 4.65 mm, the local model after penetration is generated. The crack shape is assumed to be generated after penetration. After crack penetration, the crack depth becomes 1.02 times the specimen thickness. This shape is used as the initial shape of the through crack.

The number of cycles during this crack growth process is approximately 3.9×10^4 cycles, which is negligibly smaller than the total cycles from the initial crack to the crack depth 4.65 mm, which is 1.01×10^6 cycles (3.8%).

Figure 9 represents the changes in the through crack. The number of cycles is defined as 0 when the surface crack is transformed into the through crack. Each line is the crack shape measured every 3.6×10^4 cycles. As the crack grows, the through-crack shape becomes rectangular. Figure 10 represents the changes in the stress intensity factor for each crack shape. As the crack grows, the difference of the stress intensity factors becomes small. When the number of cycles is 1.28×10^5, all stress intensity factors are nearly the same. So, it seems that the crack grows while keeping the rectangular crack shape. This is the same

result of Nam's study [13].
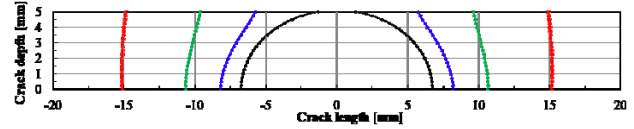
Figure 9: Changes in crack shape after penetration
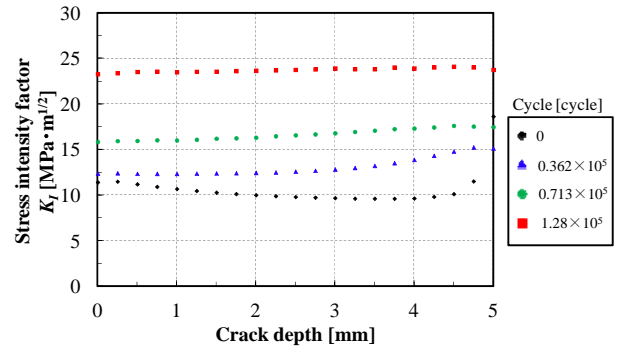
Figure 10: Changes in stress intensity factors after penetration

Figure 11 represents the relation between the crack length and the number of cycles. The lower side shows the through crack shape. where Crack length 1 and Crack length 2 are defined. As the crack grows, both crack lengths become similar. So, it is clear that the through crack grows and maintains the rectangular shape.
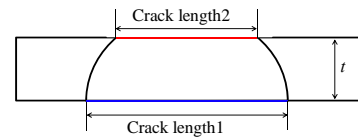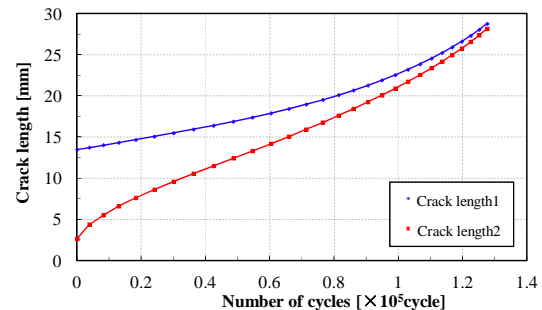
Figure 11: Relation between crack length and number of cycles

5.0 CRACK GROWTH BEHAVIOR AT WELDED PART

5.1 Numerical model

Fatigue cracks are easily generated at welded parts [14]. So, the fatigue crack growth at the welded part is analyzed. To analyze crack growth behavior from a surface crack to a through crack at the welded part, the fatigue test is the four-point bending test shown in Figure 12. The thickness of the specimen is 12 mm and

the thickness of the added plate is 30 mm. By attaching the thick added plate to the specimen, the stress of the whole specimen becomes tensile. The experimental model is symmetric, so the global mesh is a one-half model. Figure 13 shows the global mesh. The red area is the shape of the initial crack, which is located at the welded part. The initial crack length is 5.6 mm and the initial crack depth is 1.2 mm. The welded part is a triangular shape in figure 13. The crack growth magnitude is calculated by Paris' law (equation (1)). The material used in the analysis is aluminum alloy A5083. In eq.(1), C is 2.6×10^{-10} and n is 3 (unit: $MPa\sqrt{m}$).
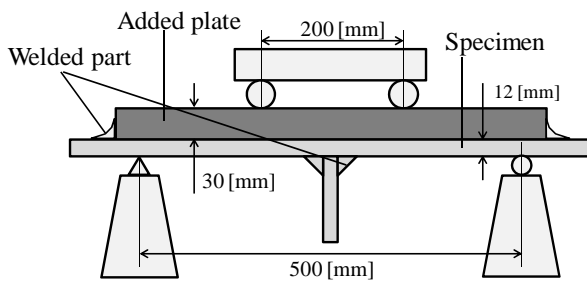
Figure 12: Four-point bending test
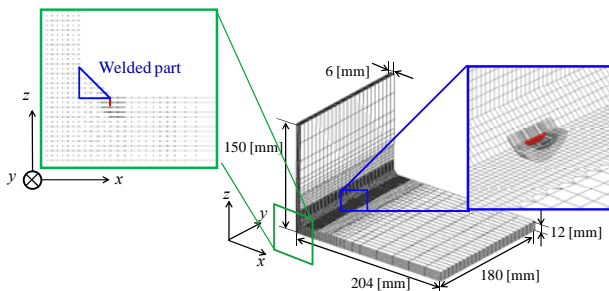
Figure 13: Dimensions of global mesh and location of the initial crack

5.2 Results of numerical simulation

Changes in the crack shape are shown in Figure 14. Each line represents the crack shape every 6.6×10^4 cycles. Due to the crack growth, the crack growing rate increases. Figure 15 shows changes in the stress intensity factors due to crack growth.

The stress intensity factors are the highest near the specimen surface due to the stress concentration at the welded part and tensile bending loading. At 1.98×10^5 cycles, the stress intensity factors near the crack depth are high. At this time, the crack depth is 11.6 mm. So, stress concentrates at the crack tip and the stress intensity factors there become high.
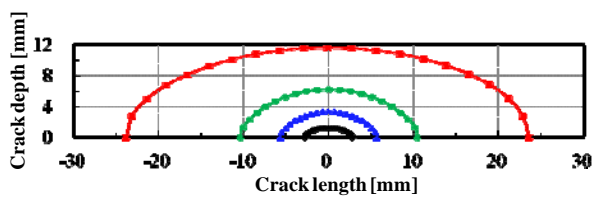
Figure 14: Crack shape before penetration
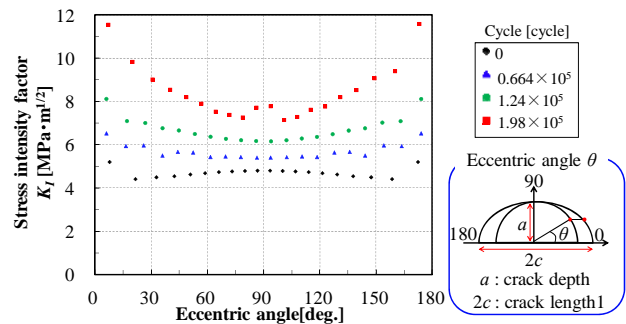
Figure 15: Stress intensity factors

Based on the final crack shape before penetration, where the crack depth is 11.6 mm, the local model after penetration is generated. The crack shape is assumed to be generated after penetration, where the crack depth becomes 1.02 times the specimen thickness. This shape is used as the initial shape of the through crack. The number of cycles during this crack growth process is approximately 5.0×10^3 cycles, which is negligibly smaller (1.5%) than the total cycles from the initial crack depth to a crack depth of 11.6 mm, which is 1.98×10^5 cycles.

By using the through crack, the crack growth behavior is analyzed after penetration. Changes in the crack shape are shown in Figure 16. The number of cycles is defined as 0 when the surface crack becomes the through crack. In Figure 16, each line is the crack shape every 1.03×10^4 cycles. As the crack grows, the crack shape becomes trapezoidal. Under cyclic tensile and bending loading, the through crack shape becomes rectangular. However, the crack shape becomes trapezoidal when the crack shape is affected by tensile bending loading.

Changes in the stress intensity factor are shown in Figure 17. Shortly after penetration, the stress intensity factors near the surface are high due to the stress concentration near the surface. As the crack grows, the difference in the stress intensity factor becomes small. In the following crack growth processes, the stress intensity factor increases in the whole crack front. It is noticed that the crack grows in a trapezoidal shape.
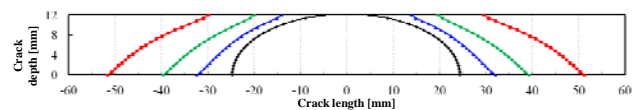
Figure 16: Crack shape after penetration
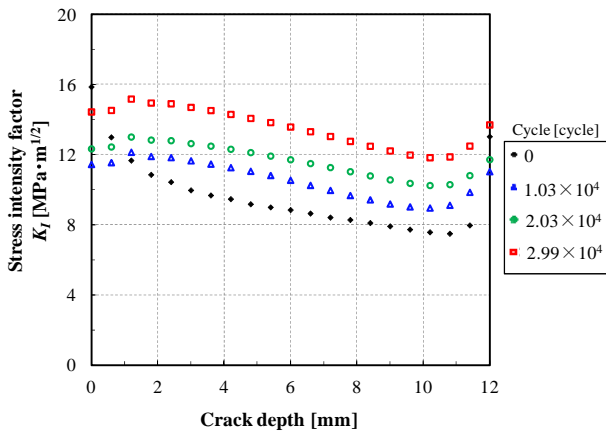
Figure 17: Stress intensity factor

Figure 18 shows the relation between crack length and number of cycles. Crack length 1 and Crack length 2 are the crack lengths of the through crack. Shortly after penetration, the crack growth rate (gradient of the curve) of Crack length 2 is faster than that of Crack length 1. As the crack grows, the gradients of each curve become the same.
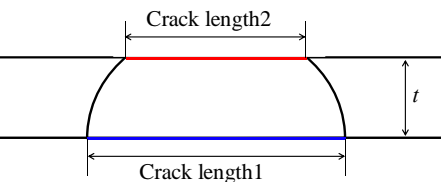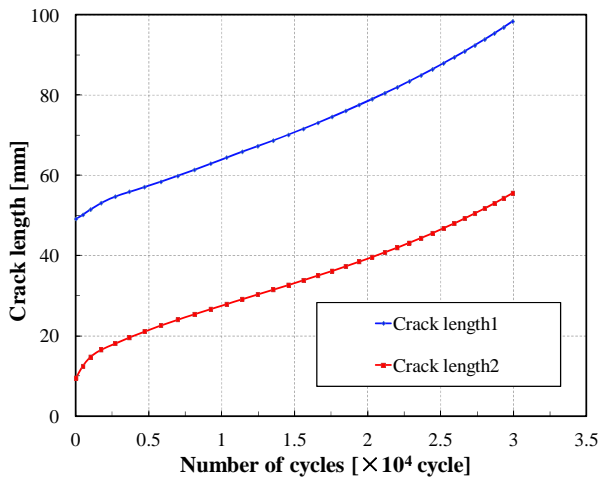
Figure 18: Crack lengths of through crack

Figure 19 shows the relation between the crack length1 and number of cycles from the surface crack to the through crack. As the crack grows, the crack growth rate becomes fast. After penetration, the crack growth rate becomes fast.
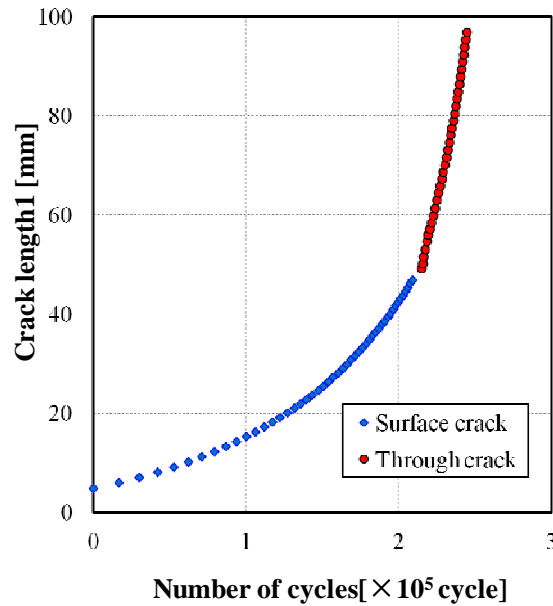
Number of cycles[$\times 10^5$ cycle]
Figure 19: Crack growth rate

6.0 CONCLUSION

It is found that when the local mesh crosses over the global mesh in the simulation by S-version FEM, the stress distributions and the stress intensity factors are hardly influenced. As a result, the through crack shape becomes rectangular under tensile cyclic load. The crack shape becomes trapezoidal under tensile bending loading after penetration. This is a reasonable result of the stress distribution.

REFERENCES

1. Nakamura, T. (2006). *Numerical Simulation of Fatigue Crack Growth for Fillet Welded Joints*, Conference Proceedings, the Japan Society of Naval Architects and Ocean Engineers, Vol. 3, pp. 355-358. (in Japanese)
2. Mori, T., Kyung, K.S., Miki, C. (1998). *The Influence of Static Strength of Steel and Weld Material on Fatigue Strength of Cruciform Filet Welded Joints*, Journal of Structural Mechanics and Earthquake Engineering, Vol. 605, No. I-45, pp. 289-293. (in Japanese)
3. Mitsui, Y., Kurobane, Y., Harada, K., Konomi, M. (1983). *Fatigue Crack Growth Behaviors at the Toe of Fillet Welded Joints under Plane Bending Load*, Journal of the Japan Welding Society, Vol. 52, No. 3, pp. 288-305. (in Japanese)
4. Nagai, K., Iwata, M., Sung-Won Kang, SOEWEIFY, (1981). *A Consideration on the Fatigue Strength of Fillet Welded Cruciform Joints of Mild Steel under Completely Reversed Bending*, Journal of the Society of Naval Architects of Japan, Vol. 149, pp. 260-267.

5. Fish, J., Markolefas, S., Guttal, R., Nayak, P. (1994). *On Adaptive Multilevel Superposition of Finite Element Meshes*, Applied Numerical Mathematics, Vol. 14, pp. 135-164.

6. Okada, H., Endoh, S., Kikuchi, M., (2005). *Application of S-Version Finite Element Method to Two Dimensional Fracture Mechanics Problems*, Transactions of the Japan Society of Mechanical Engineers Ser. A, Vol. 71, No. 704, pp. 677-684. (in Japanese)

7. Kikuchi, M., Wada, Y., Takahashi, M., Li Y. (2008). *Fatigue Crack Growth Simulation Using S-version FEM*, Transactions of the Japan Society of Mechanical Engineers Ser. A, Vol. 74, No. 742, pp. 812-818. (in Japanese)

8. Suzuki, K., Sando, A., Shimura, D., Ohtsubo, H., (2004). *Study on the Local Area Exceeding Global Area in Mesh Superposition Method*, Applied Mechanics, Vol. 7, pp. 383-389.

9. Okada, H., Higashi, M., Kikuchi, M., Fukui, Y., Kumazawa, M., (2005). *Three dimensional Virtual Crack Closure-integral Method (VCCM) with Skewed and Non-symmetric Mesh Arrangement at the Crack Front,* Engineering Fracture Mechanics, Vol. 72, pp. 1717-1737.

10. Paris, P.C., Erdogan, F. (1963). *A Critical Analysis of Crack Propagation Laws*, Journal of Basic Engineering, Trans. ASME, Ser. D, Vol. 85, pp. 528-535.

11. Lin, X.B., Smith, R.A. (1999). *Finite Element Modeling of Fatigue Crack Growth of Surface Cracked Plates Part II*: *Crack Shape Change*, Engineering Fracture Mechanics, Vol. 63, pp. 523-540.

12. Hosseini, A., MAHMOUD, M.A. (1985). *Evaluation of Stress Intensity Factor and Fatigue Growth of Surface Cracks in Tension Plates*, Engineering Fracture Mechanics, Vol. 22, pp. 957-974.

13. Nam, K.W., Matsui, K., Ando, K., Ogura, N. (1969). *The Fatigue Life and Fatigue-Crack-Through-Thickness Behavior of a Surface-Cracked Plate (3rd Report, In the Case of Combined Tensile and Bending Stress)*, Transactions of the Japan Society of Mechanical Engineers Ser. A, Vol. 55, No. 51, pp. 1740-1747. (in Japanese)

14. Tateishi, K., Kyung, K.,S., Machida F., Miki, C. (1996). *Influence of Welding Materials on Fatigue Strength of Fillet Welded Joints Made from High Strength Steel*, Journal of Structural Mechanics and Earthquake Engineering, Vol.543, No. I-36, pp. 133-140. (in Japanese)